Landfill Liners Stability Assessment using Interface Parameters

Saravanan, M.[1]. Kamon, M.[2], Faisal, H. A.[3], Katsumi T.[4], Akai, T.[5], Inui, T.[6], and Matsumoto, A.[5]

[1] *Graduate Student, Graduate School of Global Environmental Studies, Kyoto University, Kyoto, Japan*
[2]*Professor, Graduate School of Global Environmental Studies, Kyoto University, Kyoto, Japan*
[3]*Professor, Department of Civil Engineering, University Malaya, Kuala Lumpur, Malaysia.*
[4]*Associate Professor, Graduate School of Global Environmental Studies, Kyoto University, Kyoto, Japan*
[5]*Senior Research Scientist, Technology Research Institute of Osaka Prefecture, Osaka, Japan*
[6]*Assistant Professor, Graduate School of Global Environmental Studies, Kyoto University, Kyoto, Japan*

ABSTRACT: Landfill liner stability assessment using interface shear strength parameters have been a tedious testing and analysis process. The current testing procedures are based on ASTM testing guideline and basic fundamental engineering testing philosophies. Hence there is need for much ideal testing equipment which can perform the entire test series required for landfill liner parameter evaluations. The equipment are required to perform interface test between 1) soil and soil (CCLs), 2) geomembrane (HDPEs and PVC) and soil, 3) geosynthetic (GCLs) / compacted clay liners (CCLs) and soil, 4) geomembrane and geotextile, 5) geotextile and soil, 6) geotextile and geosynthetic (GCLs) / compacted clay liners (CCLs), 7) geomembrane and geosynthetic (GCLs) / compacted clay liners (CCLs). Having such high requirement and testing complexity for landfill liner system, this paper addresses the modification adopted to a large scale shear box in order to perform the above said interface tests. The modified large scale shear box was used to study interface performance of various combination of liners. Test data were compiled into a landfill model to study the stability performance of landfill liners under static and seismic loading to identify suitable liner configuration for both single and composite liner systems. The data from analysis results are compiled as quick reference guide for engineers involved in landfill liner design and maintenance. Details of laboratory test data and analysis results will be presented herewith.

1 INTRODUCTION

The world consumption of natural resources has been increasing exponentially. In Japan the consumption of resource is at 1900 million tones annually. This consumption generates waste of 600 million tones, which consist of 400 million tons of industrial waste and 50 million tons of municipal waste. Out of this 220 million tons are recycled and reused, 324 million tons are pre-treated waste for disposal. 56 million tons are disposed to landfill in Japan in year 2000. The estimated operational period of landfill site in Japan is about 6 to 10 years of operational. It becomes very difficult to build new sites in Japan cause of the syndrome “Not In My Back Yard”. The cost of new site in Tokyo could cost up to 500 million US dollars. The running cost of existing landfill site in Tokyo is at about 300 USD / m^3.

A landfill also behaves as in-situ bioreactor, where the contents undergo complex biochemical reactions. The adoption of suitable design and construction methods are essential not only to reduce design and construction cost, but also to minimize long term operation, maintenance and monitoring cost.

2 LANDFILL STABILITY

Stability of landfills has been a major concern of the present environmental geotechnical engineering community. Failures at landfill sites can be minor, however the cost of rectifications are huge. As landfill sites

generally used to contain solid waste of various kinds, which some cases can contaminate and harm the environment. Hence landfill failures could lead to serious environment pollutions. Hence engineers are required to be careful in not designing slope that exceeds the safe slope angle for liner components, internal properties and their respective interface parameters within the system. For example, an infinite slope consisting of cohesionless interfaces with no seepage, the factor of safety (F) is (Daniel et al. 1998) :

$$F = \tan \phi \ / \tan \beta \qquad (1)$$

Where, ϕ is angle of internal friction and β is slope angle. Strain incompatibility with municipal solid waste (MSW) could be another cause of stability failures. Example when failure occurs at first, in native soil, only a fraction of the MSW peak strength will be mobilized. Similar condition is also applied for geosynthetic interface and foundation soils because of their strain incompatibility with the adjacent materials in stability analysis (Hisham et al. 2000). Strain incompatibility could suggest the use of residual shear strength in stability analysis instead of peak shear strength. The soil-geomembrane interface acts as possible plane of potential instability of system under both static and seismic loading (Hoe et al. 1997). Hence environmental geotechnical engineers have strong concern about the potential instability caused by the waste containment liner system.

3 LANDFILL INTERFACE PARAMETER EVALUATION

The study of landfill liner interface parameters for stability calls for detail and compressive study of the following :

i. Landfill liner components and their interface properties
ii. Geosynthetic liner materials and their physical properties.
iii. The compacted clay liner (CCLs) interface properties with geomembrane and geosynthetic clay liners (GCLs).
iv. The interface properties of compacted clay liners (CCLs) and geosynthetic clay liners (GCLs) with native soils
v. Interface properties between CCLs, GCLs, non woven geotextile and geomembrane.
vi. Study the suitable configuration of composite liner system which could improve the liner stability without neglecting the hydraulic conductivity requirement
vii. Conduct detail stability analysis study of various configurations of landfill liner using laboratory data by limit equilibrium method.
viii. Propose recommendation for landfill stability design and installation guide for landfill liner and landfill cover to improve overall stability of landfill site by providing sufficient strain compatibility within component members

The list of interface test conducted will dependent on the configuration and material used for landfill liner system, adopted for research. The liner configuration used for research is shown in Figure 1. The research configuration consists of both single and double composite liner system. The research is still under progress to study the interface performance under saturated condition for both single and double composite liner system.

4 TESTING APPARATUS

Figures 2, 3 and 4 shows some of the typical modifications of large scale shear box adopted for the research work for three different test conditions. Namely i) Case 1 – Interface testing between geosynthetic and geosynthetic, ii) Case 2 - Interface testing between geosynthetic and soil, and iii) Case 3 - Interface testing between soil and soil. Bottom shear box size of 350 x 600mm and the top box size of 250 x 500mm were used for the test. Larger 100mm bottom box was used to define test failure of 15 % to 20% relative lateral displacement of top box dimension. However, shearing surface

contact areas were made to be similar for both top and bottom box of 250 x 500mm in size. Height adjustable bottom box base plate with spacer blocks were required to cater for variation in sample thickness and allowance for settlement or sample deformation during normal loading prior to shearing. The method also eliminates plowing kind of effect during shearing process, occurring when two different material hardness are in contact and sheared. Hence area correction method was adopted to obtain shear stresses. Constant shearing speed of 1 mm/min was used for test normal loads of 100, 200 and 300 kPa for the interface tests. ASTM D3080 -98, ASTM D5321-02 and ASTM D6243-98 was referred for the modifications.

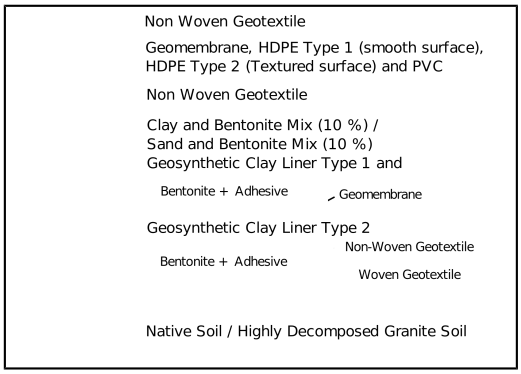

Fig. 1 : Landfill liner configuration used for the research

5 INTERFACE TEST RESULTS

In order to obtain much clear understanding of interface test results, the test data are grouped into 8 categories. The categories were made by grouping one single member interfacing with others. The categories are

i. Geotextile interfacing with geomembrane, namely HDPE Type 1 and 2, PVC and GCLs Type 1 and 2
ii. HDPE Type 1 and 2 interfacing with PVC and GCLs Type 1 and 2
iii. PVC interfacing with GCLs Type 1 and 2
iv. Geotextile and geomembrane interfacing with CCLs – Silt Bentonite mixture (100:10)
v. GCLs interfacing with CCLs – Silt Bentonite mixture (100 : 10)
vi. Geotextile and geomembrane interfacing with CCLs – Sand Bentonite mixture (100 : 10)
vii. GCLs interfacing with CCLs – Sand Bentonite mixture (100 : 10)
viii. Geotextile and geomembrane interfacing with Native Soil (Highly weathered granitic soil)

In the recorded test data, peak shear stresses were reached in wide range of strain between 2 to 15 % for the interface tests. Hence the selections of peak stresses were limited to maximum shear stresses reached within 8% strain. The obtained peak shear stresses were plotted with normal stresses to obtain peak failure envelope. Best fit linear plots were adopted in order to obtain total cohesion and total interface friction angle. The shear stress intersections were set to be either pass through axis or intercept with positive cohesion.

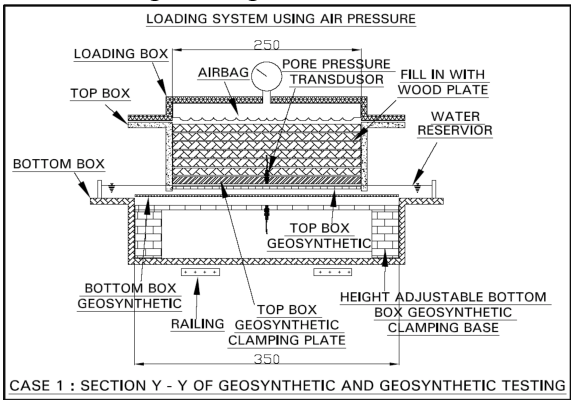

Fig. 2 : Case 1 – Modification adopted for geosynthetic and geosynthetic testing – Section Y-Y

5.1 Geotextile interfacing with geomembrane and GCLs

Using peak shear stresses within 8% strain, geotextile interfacing with PVC and GCL Type 1, (bentonite side) found to have high cohesion and frictional resistance. This could be due to plowing kind of effects created during shearing. The performance of HDPE was dominated by

textured surface HDPE. The weakest was between geotextile and geotextile from GCL Type 2 and HDPE Type 1. Details of test results are presented in Table 1 and Figure 5. In Figure 5 it shows clearly that HDPE type 1 (smooth surface) stand out of the group. Hence designers should avoid direct interface between HDPE type 1, goetextile of both woven and non woven with geotextile.

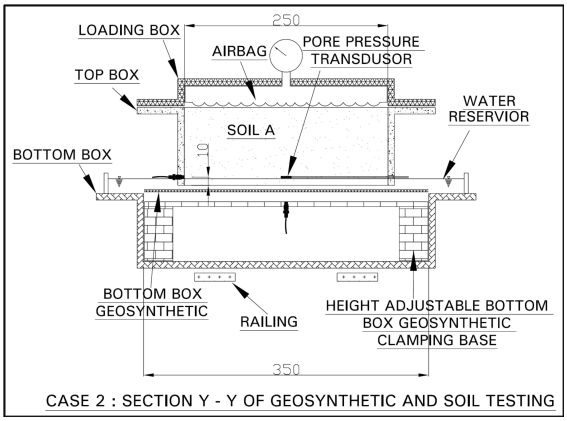

Fig. 3 : Case 2 – Modification adopted for geosynthetic and soil testing – Section Y-Y

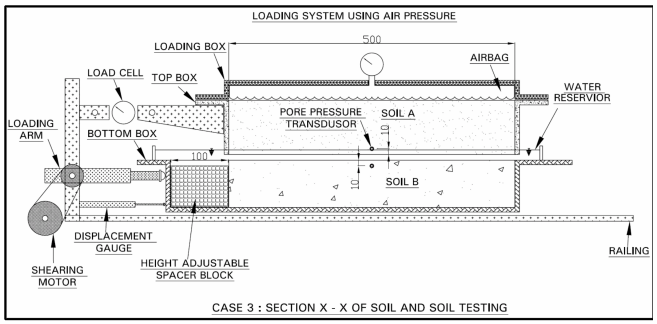

Fig. 4 : Case 3 – Modification adopted for soil and soil testing – Section X-X

Table 1 : Test results of geotextile interfacing with geomembrane

Test	Interface Parameters	Cohesion (kN/m^2)	Friction Angle (^{O})
Interface Parameters Between Geotextile and HDPE, PVC, GCLs			
Test 1A	GEOTEXTILE & HDPE Type 1	0.0	7.6
TEST 2A	GEOTEXTILE & HDPE Type 2	3.2	21.1
TEST 3A	GEOTEXTILE & PVC (Rear Side)	11.1	18.7
TEST 3C	GEOTEXTILE & PVC (Front Side)	25.7	17.1
TEST 4A	GEOTEXTILE & GCL Type 1 (Bentonite side)	12.1	17.1
TEST 4C	GEOTEXTILE & GCL Type 1 (HDPE Side)	0.0	21.8
TEST 5A	GEOTEXTILE & GCL Type 2 (Non Woven Site)	1.5	15.1
TEST 5C	GEOTEXTILE & GCL Type 2 (Woven Side)	10.5	14.8

5.2 HDPE Type 1 and 2 interfacing with GCLs

The performances of HDPEs were clearly distinguished between the case of smooth and textured surface. The fictional contribution of smooth surface HDPE was between 7 to 9 degrees. The textured surface of HDPE contributes frictional resistance in the range of 19 to 26 degree with increment of 10 to 15 in friction angle as compared to smooth surface HDPE. Details of the test results are presented in Table 2 and Figure 6.

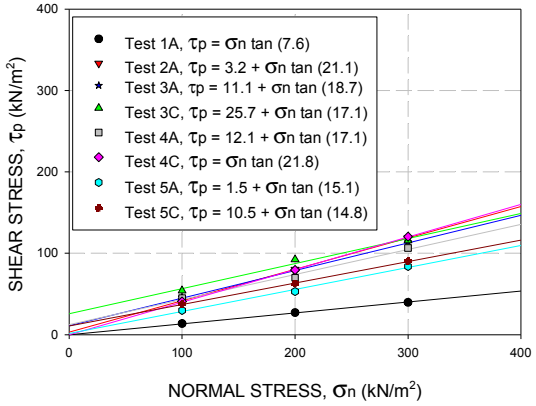

Fig. 5 : Summary of peak failure envelopes for geotextile interfacing with geomembrane.

Table 2 : Test results of HDPE Type 1 and 2 interfacing with GCLs

Test	Interface Parameters	Cohesion (kN/m^2)	Friction Angle (^{O})
Interface Parameters Between HDPEs and PVC, GCLs			
TEST 6A	HDPE Type 1 & GCL Type 1 (Bentonite Side)	0.0	9.1
TEST 6C	HDPE Type 1 & GCL Type 1 (HDPE Side)	2.2	8.9
TEST 7A	HDPE Type 1 & GCL Type 2 (Non Woven Side)	2.2	7.8
TEST 7C	HDPE Type 1 & GCL Type 2 (Woven Side)	2.4	9.3
TEST 8A	HDPE Type 2 & GCL Type 1 (Bentonite Side)	28.8	19
TEST 8C	HDPE Type 2 & GCL Type 1 (HDPE Side)	0.0	19.9
TEST 9A	HDPE Type 2 & GCL Type 2 (Non Woven Side)	10.2	25.7
TEST 9C	HDPE Type 2 & GCL Type 2 (Woven Side)	2.1	23.2

These results also isolate HDPE type 1 which has low interface properties.

5.2 PVC interfacing with GCLs

The performances of PVC with GCLs were relatively consistent with interface test results,

within narrow range of differences. The fictional contribution of PVC was between 15 to 18 degree, while cohesions were in the range of 10 to 24 kN/m^2. The performance of woven geotextile was much higher in term of frictional resistance as compared to non woven geotextile of the GCL type 2. Details of the test results are presented in Table 3 and Figure 7 respectively.

Fig. 6 : Summary of peak failure envelopes for HDPE Type 1 and 2 interfacing with GCLs.

Table 3 : Test results of PVC interfacing with GCLs

Test	Interface Parameters	Cohesion (kN/m^2)	Friction Angle (^{O})
Interface Parameters Between PVC and GCLs			
TEST 10A	PVC (Rear Side) & GCL Type 1 (Bentonite Side)	17.6	18.1
TEST 11A	PVC (Rear Side) & GCL Type 2 (Non Woven Side)	17.2	15.3
TEST 11C	PVC (Rear Side) & GCL Type 2 (Woven Side)	14.7	18.1
TEST 11E	PVC Front Side & GCL Type 2 (Non Woven Side)	10.0	17.4
TEST 11G	PVC (Front Side) & GCL Type 2 (Woven Side)	24.0	18.4

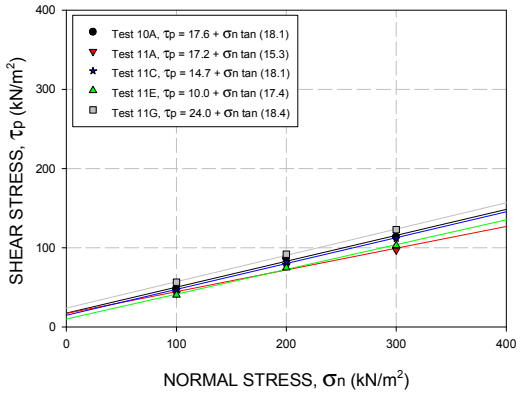

Fig. 7 : Summary of peak failure envelopes for PVC interfacing with GCLs

PVC tends to provide reliable performance on both sides of the surface.

5.4 Silt bentonite (100 : 10) interfacing with geosynthetics

The performances of silt bentonite mixture (100 : 10) with geosynthetics were relatively consistent with interface test results within narrow range of differences. Only fictional contribution was exhibited without cohesion. The performance of geotextile and HDPE type 1 was the lowest with fiction angle of 15 degrees. HDPE type 2 and PVC provide high and relatively consistent frictional resistance. Details of the test results are presented in Table 4 and Figure 8 respectively.

Table 4 : Test results of silt bentonite (100 : 10) interfacing with geosynthetics

Test	Interface Parameters	Cohesion (kN/m^2)	Friction Angle (^{O})
Interface Parameters Between Geosynthetic and Silt Bentonite Mixture (100 : 10) CCL			
TEST 12A	GEOTEXTILE & SILT BENTONITE Mix(100 : 10)	0.0	15.3
TEST 13A	HDPE Type 1 & SILT BENTONITE Mix (100 : 10)	0.0	15.4
TEST 14A	HDPE Type 2 & SILT BENTONITE Mix (100 : 10)	0.0	24.2
TEST 15A	PVC (Rear Side) & SILT BENTONITE Mix (100 : 10)	0.0	22.2
TEST 15C	PVC (Front Side) & SILT BENTONITE Mix (100 : 10)	0.0	20.0

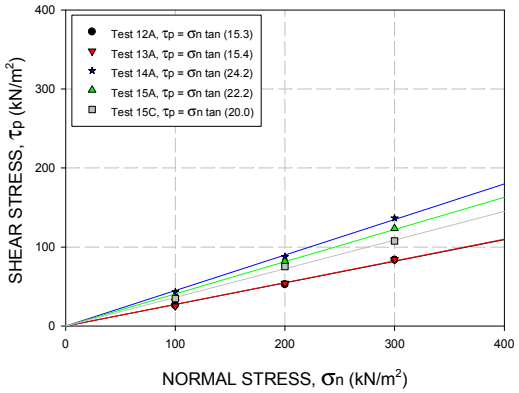

Fig. 8 : Summary of peak failure envelopes for Silt bentonite (100 : 10) interfacing with Geosnthetics

Eventhough HDPE Type 1 and geotextile had low frictional resistance, the interface values are higher as compared to direct interface

between geotextile and HDPE Type 1. Hence it is proposed to sandwich HDPE Type 1 or geomembrane in general within compacted clay liner (CCL) , shown in Figure 9, rather than placing on top of geotextile, as shown in Figure 10. Precautions are required to avoid damages on geomembrane during installation of compacted clay liner (CCL) due to direct contact. It is recommended to allow for some sacrificial thickness on geomembrane to resists major or microscopic puncture.

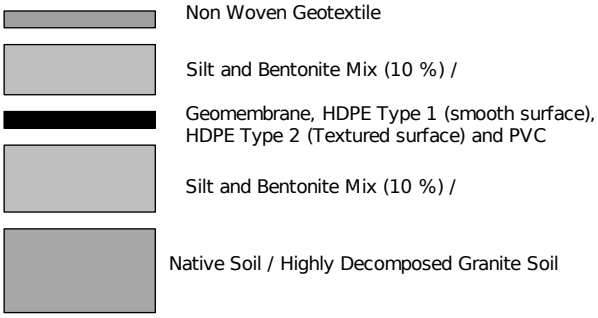

Fig. 9 : Single composite liner configuration

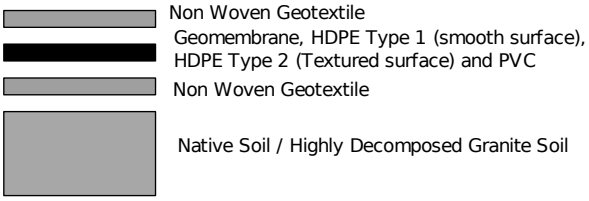

Fig. 10 : Single membrane liner configuration

5.5 Silt bentonite (100 : 10) interfacing with GCLs Type 1 and 2

The performances of silt bentonite mixture (100 : 10) with geosynthetics clay liners (GCL) were relatively consistent with interface test results within narrow range of differences. Higher cohesion and lower frictional contribution was observed with GCL type 1 (bentonite side). Higher fiction was observed in the case of GCL type 1 (HDPE side) and GCL type 2 (woven side). In general both GCLs sides contributed high frictional resistance with silt bentonite (100 : 10). Details of the test results are presented in Table 5 and Figure 11 respectively. GCL test results were very much similar of those from HDPE Type 2 and PVC interface with silt bentonite.

Table 5 : Test results of silt bentonite (100 : 10) interfacing with geosynthetics

Test	Interface Parameters	Cohesion (kN/m^2)	Friction Angle (^{O})
Interface Parameters Between GCLs and Silt Bentonite Mixture (100 : 10) CCL			
TEST 17A	GCL Type 1 (Bentonite Side) & SILT BENTONITE Mix (100 : 10)	13.9	17.0
TEST 17C	GCL Type 1 (HDPE Side) & SILT BENTONITE Mix (100 : 10)	0.0	22.6
TEST 18A	GCL Type 2 (Non Woven Side) & SILT BENTONITE Mix (100 : 10)	6.2	20.8
TEST 18C	GCL Type 2 (Woven Side) & SILT BENTONITE Mix (100 : 10)	1.4	21.4

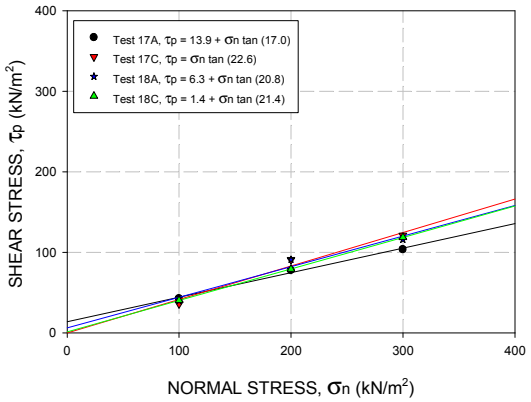

Fig. 11 : Summary of peak failure envelopes for Silt bentonite (100 : 10) interfacing with GCLs

5.6 Sand bentonite (100 : 10) interfacing with geosynthetics

The performances of sand bentonite mixture (100 : 10) with geosynthetics were covered in wide range of friction angle. Only fictional contribution was exhibited without cohesions. The performance of geotextile and HDPE type 1 were the lowest with fiction angle of 13 to 15 degrees. HDPE type 2 and PVC provide high and relatively similar frictional resistance. However friction angle of PVC front side (smooth surface) was as low as geotextile friction angle. Details of the test results are presented in Table 6 and Figure 12 respectively. The performance of silt bentonite mixture (100 : 10) and sand bentonite mixture (100 : 10) with geosynthetics were consistent. However the friction contribution of sand bentonite was marginally lower compared to silt bentonite mixture (100 : 10). Initial prediction, sand was believed to provide higher frictional resistance as compared to silt. However the test results were not as predicted due to the presents of bentonite in sand and higher damage were created on interfacing member during shearing by sand.

Table 6 : Test results of sand bentonite (100 : 10) interfacing with geosynthetics

Test	Interface Parameters	Cohesion (kN/m^2)	Friction Angle (^{o})
Interface Parameters Between Geosynthetic and Sand Bentonite Mixture (100 : 10) CCL			
TEST 19A	GEOTEXTILE & SAND BENTONITE Mix (100 : 10)	0.0	15.8
TEST 20A	HDPE Type 1 & SAND BENTONITE Mix (100 : 10)	0.0	13.8
TEST 21A	HDPE Type 2 & SAND BENTONITE Mix (100 : 10)	0.0	24.5
TEST 22A	PVC (Rear Side) & SAND BENTONITE Mix (100 : 10)	0.0	19.8
TEST 22C	PVC (Front Side) & SAND BENTONITE Mix (100 : 10)	0.0	16.9

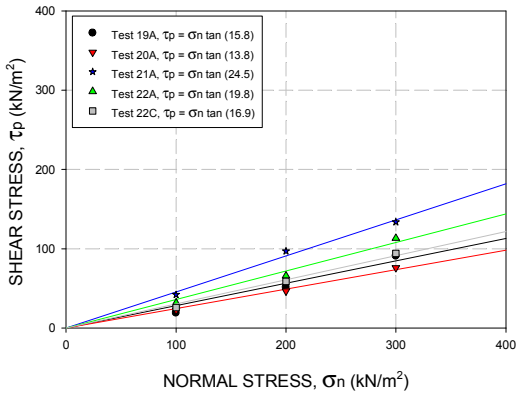

Fig. 12 : Summary of peak failure envelopes for Silt bentonite (100 : 10) interfacing with geosynthetics

5.7 Sand bentonite (100 : 10) interfacing with GCLs Type 1 and 2

The performances of sand bentonite mixture (100 : 10) with GCL type 1 and 2 were covered with narrow minimum and maximum range. Cohesion was not contributed in the case of GCL type 2. GCL type 1 (HDPE side) has the lowest friction angle. GCL type 1 (bentonite side) and GCL type 2 frictional resistances were similar for both sides. Details of the test results are presented in Table 7 and Figure 13.

Table 7 : Test results of sand bentonite (100 : 10) interfacing with geosynthetics

Test	Interface Parameters	Cohesion (kN/m^2)	Friction Angle (^{o})
Interface Parameters Between GCLs and Sand Bentonite Mixture (100 : 10) CCL			
TEST 24A	GCL Type 1 (Bentonite Side) & SAND BENTONITE Mix (100 : 10)	6.5	17.6
TEST 24C	GCL Type 1 (HDPE Side) & SAND BENTONITE Mix (100 : 10)	14.7	13.7
TEST 25A	GCL Type 2 (Non Woven Side) & SAND BENTONITE Mix (100 : 10)	0.0	22.6
TEST 25C	GCL Type 2 (Woven Side) & SAND BENTONITE Mix (100 : 10)	0.0	21.9

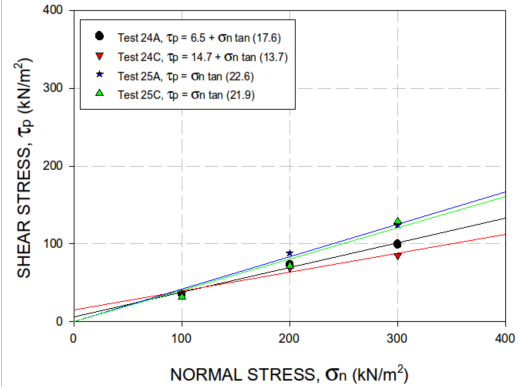

Fig. 13 : Summary of peak failure envelopes for Sand bentonite (100 : 10) interfacing with GCLs Type 1 and 2

As compared to performance silt bentonite with GCL Type 1 and 2, sand bentonite had better cohesional contribution and with lower frictional resistance. In general silt bentonite had much better interface properties as compared to sand bentonite. However careful case by case selection is required.

5.8 Native soil interfacing with geosynthetics

The performances of native soil with geosynthetics were covered in wide range of friction angle. Only fictional contribution was exhibited without cohesions. The performance of geotextile, HDPE type 1 and PVC (rear side) were the lowest with fiction angle of 15 to 19 degrees. HDPE type 2 provides high frictional resistance. Details of the test results are presented in Table 8 and Figure 14 respectively.

Table 8 : Test results of native soil interfacing with geosynthetics

Test	Interface Parameters	Cohesion (kN/m^2)	Friction Angle (^{0})
Interface Parameters Between Geosynthetic and Native Soil (HW Granitic Soil)			
TEST 26A	GEOTEXTILE & NATIVE SOIL	0.0	17.8
TEST 27A	HDPE TYPE 1 & NATIVE SOIL	0.0	15.6
TEST 28A	HDPE TYPE 2 & NATIVE SOIL	0.0	23.1
TEST 29A	PVC (Rear) & NATIVE SOIL	0.0	18.7

By comparing CCLs and native soil, the interface of geotextile and HDPE Type 1 contribute higher interface property as compared to CCLs. Lower interfaces were observed for HDPE Type 2 and PVC (rear side) with native soil as compared to CCLs. These could be higher damages created by native soil especially on texture of HDPE Type 2.

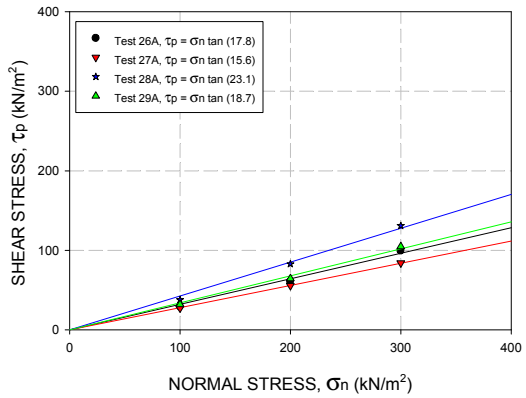

Fig. 14 : Summary of peak failure envelopes for native soil interfacing with geosynthetics

6 SIMPLIFIED FACTOR OF SAFETY ASSESSMENT

In order to study into the influence of normal loads on liner factor of safety. Two simple cross sections were adopted. The cross sections are :

a Case 1 – Landfill of 30m high (H) and 135m width (W), with side slopes of 1V : 1H, 1V : 2H, 1V : 3H, classified as safe under static condition. W/H = 4.5. As shown in Figure 15

b Case 2 – Landfill of 10m high (H) and 135m width (W), with side slopes of 1V : 1H, 1V : 2H, 1V : 3H, classified as very safe under static condition. W/H = 13.5. As shown in Figure 16

In the simplified approach the adopted assumption is that interface failure is within the plane of interface and without intercepting other member components or other interface plane. Hence the analysis failures modes were two part wedge and three part wedge mode for cover slopes and bottom liners respectively. Table 9 list out the analysis cases considered with static and seismic condition.

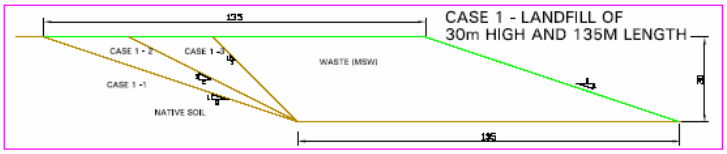

Fig. 15 : Case 1 – Landfill of 30m high (H) and 135m width (W), W/H = 4.5

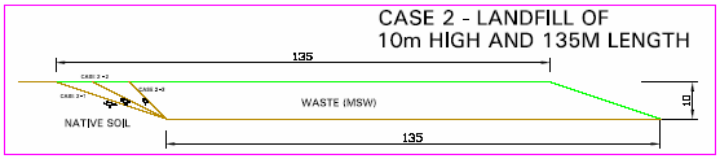

Fig. 16 : Case 2 - Landfill of 30m high (H) and 120m width (W), W/H = 13.5

6.1 Factor of safety computation

Factor of safety computation for liner stability was based on limit equilibrium approach. At limit equilibrium all points along the sliding plane are assumed to be near failure. The factor of safety is defined as the ratio of resisting forces to driving forces,

$$\text{Factor of Safety } (F) = \frac{Total Driving Force}{Total\ \text{Re}\ sisting Force}$$

Table 9 : List of cases analysed are listed below

CASES	DESCRIPTION
Case 1A - 1	Slope height of 30m with 135m length with back slope angle of 3H:1V and seismic coefficient of 0.00
Case 1B - 1	Slope height of 30m with 135m length with back slope angle of 3H:1V and seismic coefficient of 0.10
Case 1C - 1	Slope height of 30m with 135m length with back slope angle of 3H:1V and seismic coefficient of 0.15
Case 1D – 1	Slope height of 30m with 135m length with back slope angle of 3H:1V and seismic coefficient of 0.20
Case 1E - 1	Slope height of 30m with 135m length with back slope angle of 3H:1V and seismic coefficient of 0.25
Case 1A – 2	Slope height of 30m with 135m length with back slope angle of 2H:1V and seismic coefficient of 0.00
Case 1B – 2	Slope height of 30m with 135m length with back slope angle of 2H:1V and seismic coefficient of 0.10
Case 1C – 2	Slope height of 30m with 135m length with back slope angle of 2H:1V and seismic coefficient of 0.15
Case 1D – 2	Slope height of 30m with 135m length with back slope angle of 2H:1V and seismic coefficient of 0.20
Case 1E - 2	Slope height of 30m with 135m length with back slope angle of 2H:1V and seismic coefficient of 0.25
Case 1A – 3	Slope height of 30m with 135m length with back slope angle of 1H:1V and seismic coefficient of 0.00
Case 1B – 3	Slope height of 30m with 135m length with back slope angle of 1H:1V and seismic coefficient of 0.10
Case 1C – 3	Slope height of 30m with 135m length with back slope angle of 1H:1V and seismic coefficient of 0.15
Case 1D – 3	Slope height of 30m with 135m length with back slope angle of 1H:1V and seismic coefficient of 0.20
Case 1E - 3	Slope height of 10m with 135m length with back slope angle of 1H:1V and seismic coefficient of 0.25
Case 2A - 1	Slope height of 10m with 135m length with back slope angle of 3H:1V and seismic coefficient of 0.00
Case 2B - 1	Slope height of 10m with 135m length with back slope angle of 3H:1V and seismic coefficient of 0.10
Case 2C - 1	Slope height of 10m with 135m length with back slope angle of 3H:1V and seismic coefficient of 0.15
Case 2D – 1	Slope height of 10m with 135m length with back slope angle of 3H:1V and seismic coefficient of 0.20
Case 2E - 1	Slope height of 10m with 135m length with back slope angle of 3H:1V and seismic coefficient of 0.25
Case 2A – 2	Slope height of 10m with 135m length with back slope angle of 2H:1V and seismic coefficient of 0.00
Case 2B – 2	Slope height of 10m with 135m length with back slope angle of 2H:1V and seismic coefficient of 0.10
Case 2C - 2	Slope height of 10m with 135m length with back slope angle of 2H:1V and seismic coefficient of 0.15
Case 2D – 2	Slope height of 10m with 135m length with back slope angle of 2H:1V and seismic coefficient of 0.20
Case 2E – 2	Slope height of 10m with 135m length with back slope angle of 2H:1V and seismic coefficient of 0.25
Case 2A – 3	Slope height of 10m with 135m length with back slope angle of 1H:1V and seismic coefficient of 0.00
Case 2B – 3	Slope height of 10m with 135m length with back slope angle of 1H:1V and seismic coefficient of 0.10
Case 2C – 3	Slope height of 10m with 135m length with back slope angle of 1H:1V and seismic coefficient of 0.15
Case 2D – 3	Slope height of 10m with 135m length with back slope angle of 1H:1V and seismic coefficient of 0.20
Case 2E - 3	Slope height of 10m with 135m length with back slope angle of 1H:1V and seismic coefficient of 0.25

Resisting / Passive forces were made up of forces such as shear strength of the failure plane and other stabilizing forces acting on the wedge. Active forces consist of down-slope component weight of the sliding block, forces such as those generated by seismic acceleration or by water pressures acting on faces of the block, and external forces on the upper slope surface. By using Mohr Coulomb criteria

$$\tau = c + \sigma_n \tan\phi$$

$$F = \frac{cL + W\cos\alpha\tan\phi}{W\sin\alpha}$$

L = Length of failure plane

τ = Total shear strength

c = Total cohesion

W = Total weight acting on the failure plane

α, β = Side slope angle or cover slope

ϕ = Total friction angle

σ_n = Total normal stress on failure plane

F = Factor of safety

The above equation is simplified further by computing fictional and cohesion contribution individually.

Friction Contribution

$$F = \frac{\tan\phi}{\tan\alpha}$$

Cohesion Contribution

$$F = \frac{cL}{W\sin\alpha}$$

6.3 Seismic Influence of Factor of Safety

Seismic effects were also analysis by performing limit equilibrium analysis where the forces induced by earthquake accelerations were treated as horizontal force. Vertical forces were also caused by earthquake however the forces were not computed in the analysis. Where horizontal force (F_h), due to earthquake assumed to act through centre of gravity of soil mass involved to predict the failure. It is assumed that:

$F_h = kw = k\,mg$

Where, m is the mass of the soil and k is seismic coefficient. Thus the seismic coefficient k is measurement of earthquake acceleration in terms of g. The sample calculation is shown in Table 10 and liner computation model is shown in Figure 17.

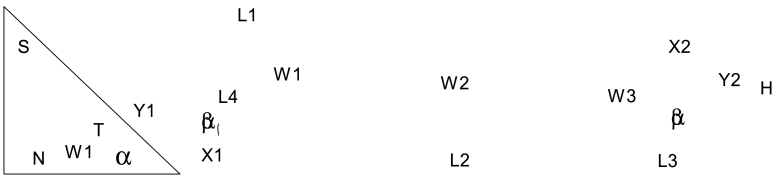

Fig. 17 : Liner computation model

FOS from Friction = $FOS_f = \tan\phi * (P/A)$

FOS from Cohesion = $FOS_C = \tan\phi * (L/A)$

Total FOS = $FOS_F + FOS_C$

Figure 18, shows the typical performance of interface factor of safety with total FOS computed. Figure 19, shows a specific interface case study of Test 3A (interface between geotextile and PVC (rear side), where

drastic drop in factor of safety with seismic coefficient, even for the case of very stable slope under static condition. The rapid drop in total FOS under seismic condition indicate that all slope or landfill configurations are critically venerable to have interface failure during earthquake. Hence in order to understand, predict and monitor the continuous trend factor of safety during filling and maintenance, factor of safeties were computed individually based on frictional and cohesion contribution. Figure 20 and 21 shows the invidual plots of factor of safety based on friction and cohieson respectively.

Table 10 : Model computations are as below

Passive		Active	
(W1)*cos α	, P1 kN/m	(W1)*sin α	, A1 kN/m
W2	, P2 kN/m		
W3	, P3 kN/m	Seismic active	
		W1 * (k)	, A2 kN/m
Total Passive	P kN/m	W2 * (k)	, A3 kN/m
		W3 * (k)	, A4 kN/m
Total Length			
L2 + L3 + L4	, L m	Total Active	A kN/m
Friction	Passive / Active or P/A		
Cohesion	L/(Active) or L/A		

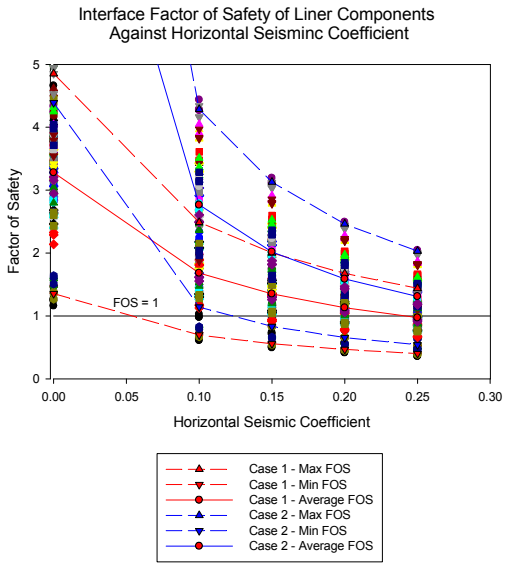

Fig. 18 : Performance of interface factor of safety of liner components against horizontal seismic coefficient.

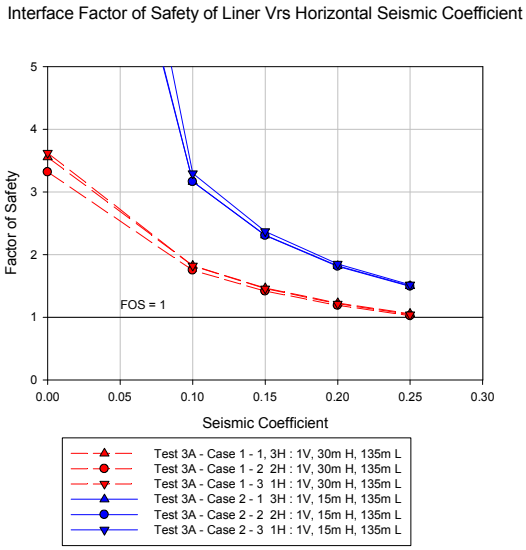

Fig. 19 : Specific interface case study of Test 3A.

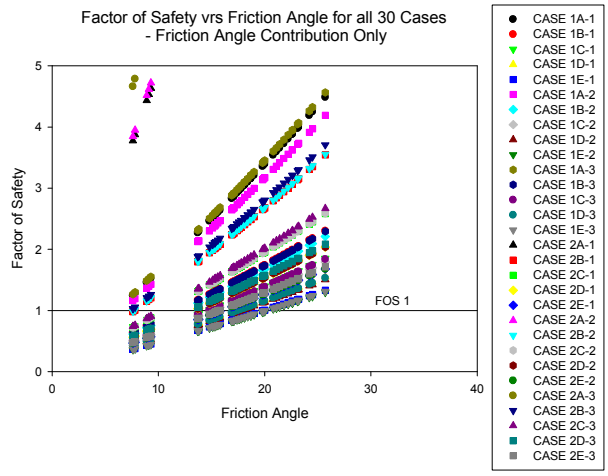

Fig. 20 : Interface factor of safety based on frictional contribution only.

The frictional contribution of factor of safety tends to have expotional increment with friction angle. Where the higher the value of passive resistance against active forces (P/A) higher was the factor of safety, as shown in Figure 22. Similar case was also observed in Figure 23, where linear increment of factor of safety was obtained with increment in cohesion. The incorporated plot of Length of interface / Active forces (L/A) allows estimation of factor of safety based on cohesion parameters.

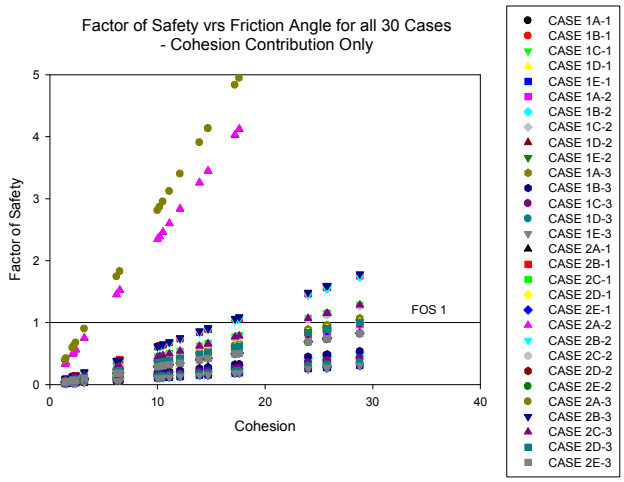

Fig. 21 : Interface factor of safety based on cohesion contribution only.

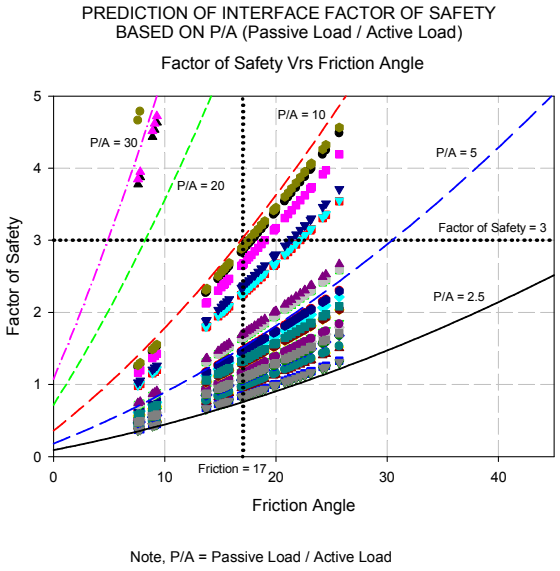

Fig. 22 : Interface factor of safety based on friction with P/A coefficient incoperated.

Example of factor of safety prediction, Say interface parameters of

$$\tau = 30 + \sigma_n \tan 17$$

In order to obtain landfill total factor of safety of 3, only by frictional contribution the Passive/Active cohesion should be 10 and by cohesion the Length of interface / Active forces (L/A) should be 0.1. In the case of combining both frictional and cohesion a total factor of safety of 6 is obtained. The influence of seismic coefficient can be computed using the model calculation method shown in Table 10.

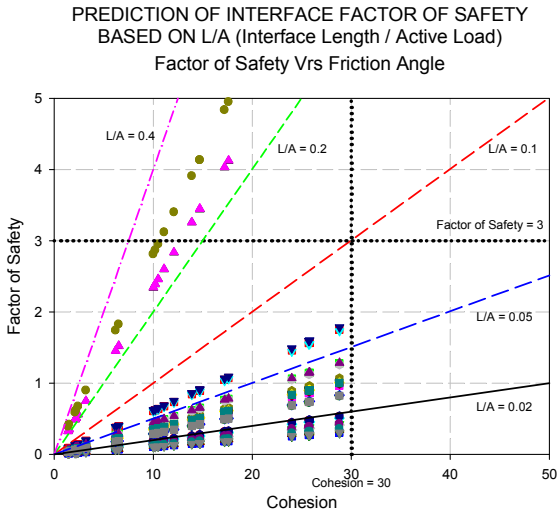

Fig. 23 : Interface factor of safety based on cohesion with L/A coefficient incorporated.

6.3 Advantage of Proposed FOS Prediction Method

1. Will be quick reference guide for engineers in selecting liner materials based on interface test results
2. Can obtain initial estimation of FOS based on site or back slope conditions
3. Useful to design appropriate anchorage methods for liners to obtain adequate FOS
4. Perform continuous monitoring of FOS of landfill site with filling work in progress.
5. Assist in organising sequential filling in order to maintain adequate FOS for both static and seismic condition
6. If FOS is found to be not adequate appropriate steps can be taken immediately to avoid sudden failures
7. Useful for site engineers to coordinate the work in progress safely.

7 DISCUSSIONS AND CONCLUSIONS

Engineers are required to balance out the active and passive resistance force (P/A), in order not to have sudden and drastic drop in factor of safety during earthquake. Hence it is vital to perform continuous factor of safety assessment during on going filling works to ensure the landfill site is stable at all time to resist seismic failure. Based on Figure 22 as the friction angle reduces, the rate of factor of safety reduction is rapid in the case of higher P/A values. This indicates that not all save slope are actually stable under seismic condition, when it comes to interface induced failure.

8 ACKNOWLEDGEMENTS

The authors wish to extend special thanks to: all the individuals and institutions involved directly and indirectly by providing financial and material support for this research work.

9 REFERENCES

ASTM D3080–98 “Standard Test Method for Direct Shear Test of Soils Under Consolidated Drained Conditions”. Annual Book of ASTM Standards, Vol. 04.08. pp. 347 – 352.

ASTM D5321–02 “Standard Test Method for Determining the Coefficient of Soil and Geosynthetic or Geosynthetic and Geosynthetic Friction by the Direct Shear Method”. Annual Book of ASTM Standards, Vol. 04.13. pp. 123-129.

ASTM D6243–98 “Standard Test Method for Determining the Internal and Interface Shear Resistance of Geosynthetic Clay Liner by the Direct Shear Method”. Annual Book of ASTM Standards, Vol. 04.13. pp. 287-293.

Daniel D. E., Koerner R. M., Bonaparte R., Landreth R. E., Carson D. A. and Scranton H. B. (July 1998) “Slope Stability Of Geosynthetic Clay Liner test Plots”, Journal of Geotechnical and Geoenvironmental Engineering, pp. 628-637.

Hisham T. Eid, Timothy D. Stark, W. Douglas Evans, and Paul E. Sherry (May 2000) “Municipal Solid Waste Slope Failure. I Waste and Foundation Soil Properties”, Journal of Geotechnical and Geoenvironmental Engineering, pp. 397-407.

Hoe I. Ling and Dov Leshchinsky, (February 1997) “Seismic Stability And Permanent Displacement of Landfill Cover Systems”, Journal of Geotechnical and Geoenvironmental Engineering, pp. 113-122.